JOC Article

Nitrosation Chemistry of Pyrroline, 2-Imidazoline, and 2-Oxazoline: Theoretical Curtin−Hammett Analysis of Retro-Ene and Solvent-Assisted C−X Cleavage Reactions of α-Hydroxy-*N*-Nitrosamines

Hong Wu, Richard N. Loeppky, and Rainer Glaser*

Department of Chemistry, University of Missouri-Columbia, Columbia, Missouri 65211

glaserr@missouri.edu

Received April 27, 2005

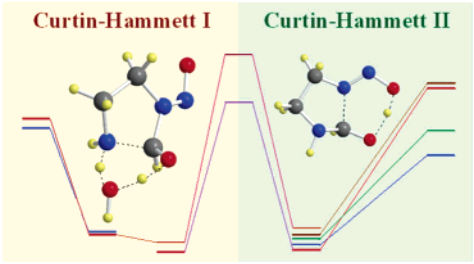

The results are presented of a theoretical study of the nitrosation chemistry of pyrroline **1** (X = CH_2), imidazoline **2** (X = NH), and 2-oxazoline **3** (X = O). Imines **1**−**3** are converted to the α-hydroxy-*N*-nitrosamines **7**−**9** via the *N*-nitrosoiminium ions **4**−**6**. The NN-*cis* isomers of **7**−**9** may undergo retro-ene reactions to the δ-oxoalkyl diazotic acids **10**−**12**. With the opportunity for microsolvation, C−X cleavage becomes possible for **8** and **9** and leads to the formation of *N*-(2-aminoethyl)- and *N*-(2-hydroxyethyl)-*N*-nitrosoformamides **15** and **16**, respectively. The NN-isomerization barriers are comparable to the barriers for the ring-opening reactions, and the consideration of two Curtin−Hammett scenarios is required: CH-**I** for the NN-*trans*-rotamers of **7**−**9** to undergo C−X cleavage or NN-isomerization and CH-**II** for the NN-*cis*-rotamers to undergo C−X cleavage, C−N cleavage, or NN-isomerization. We determined all stereoisomers of the substrates, the products, and of all transition states structures for the retro-ene reactions of **7**−**9**, the C−X cleavages of microsolvated **8** and **9**, and the NN-isomerizations of **8** and **9**. The potential energy surfaces were explored at the B3LYP/6-31G** level, and the results are discussed with emphasis on the comparison of the kinetics and thermodynamics of C−N versus C−X cleavage. The study shows all decompositions to be very fast with activation barriers below 21 kcal·mol^{-1}, and the comparitive analysis predicts that the chemical toxicologies of **1** and **3** should be similar and remarkably different from that of **2**.

Introduction

N-Nitrosamines and related *N*-nitroso compounds are one important class of naturally occurring carcinogens. These chemical carcinogens damage DNA by alkylation of the DNA bases, and the reactive species are the diazonium ions or carbonium ions resulting from the decomposition of the *N*-nitroso compounds.[1] Some *N*-nitrosamines are contained in the human diet and any of these toxicological concerns can be addressed by food quality control and dietary restrictions. More disconcerting are the results of recent studies that have demonstrated that such compounds can be formed by endogenous nitrosation.[2] *N*-Nitrosamines are latent carcinogens and require cytochrome P450 mediated α-oxidation for their conversion into the active carcinogens, the α-hydroxy-*N*-nitrosamines.[3] The decomposition pathways of alkyl-*N*-nitrosamines have been intensively studied both experimentally and theoretically,[4] and cyclic *N*-nitrosamines have received increasing attention.[5−7] In this

(1) (a) Blans, P.; Fishbein, J. C. *Chem. Res. Toxicol*. **2004**, *17*, 1531. (b) Blans, P.; Fishbein, J. C. *Chem. Res. Toxicol*. **2000**, *13*, 431. (c) Lewis, D. F. V.; Brantom, P. G. Ioannides, C.; Walker, R.; Parke, D. V. *Drug Meta. Rev*. **1997**, *29*, 1055. (d) *Nitrosamines and Related N-Nitroso Compounds. Chemistry and Biochemistry*; Loeppky, R. N., Michejda, C. N., Eds.; ACS Symposium Series No. 533; American Chemical Society: Washington, DC, 1994. (e) *Chemistry and Biology of N-Nitroso Compounds*; Lijinsky, W., Cambridge University Press: Cambridge, U.K., 1992. (f) Brunnemann, K. D.; Hecht, S. S.; Hoffmann, D. N. *J. Toxicol. Clin. Toxicol*. **1982**, *19*, 661. (g) Magee, P. N.; Barnes, J. M. *Adv. Cancer Res*. **1967**, *10*, 163.

(2) Huang, Y.; Ji, J.; Hou, Q. *Mutat. Res*. **1996**, *358*, 7.

10.1021/jo050856s CCC: $30.25
Published on Web 07/23/2005

SCHEME 1. Overview

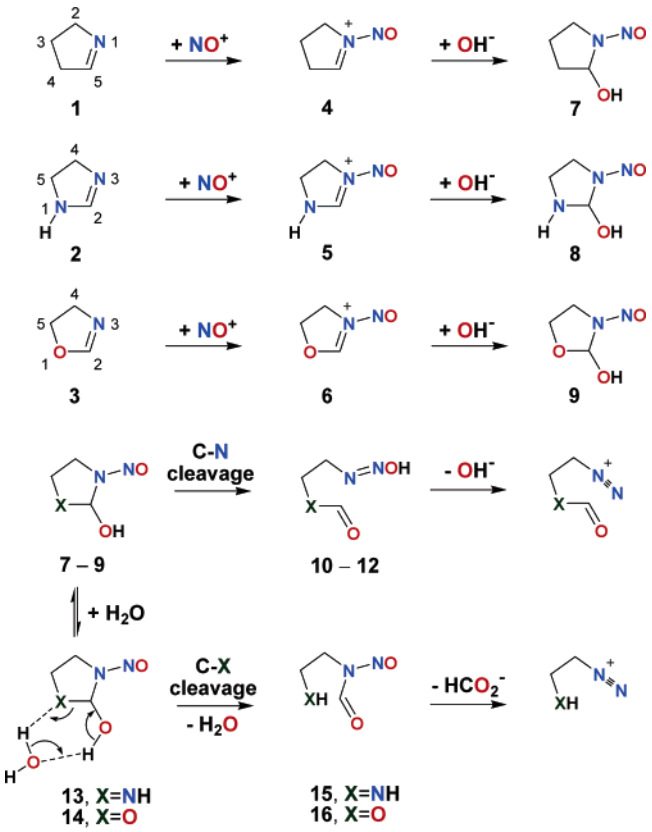

context, we focus here on the elucidation of the possible role of nitrosation of compounds with C=N double bonds in the generation of cell-damaging electrophiles. We recently reported on the nitrosation of the C=N bonds of acyclic secondary and tertiary amidines.[8]

In the present paper, we are discussing the nitrosation chemistry of three cyclic imines: Δ^1-pyrroline **1** (X = CH_2), 2-imidazoline **2** (X = NH), and 2-oxazoline **3** (X = O). These imines occur in a number of drugs,[9] and it is our postulate that endogenous nitrosation might convert these imines into potent carcinogens (Scheme 1). Imines **1**−**3** first are activated by conversion to the α-hydroxynitrosamines **7**−**9** via stepwise and acid-catalyzed addition of HO−NO via the *N*-nitrosoiminium ions **4**−**6**. The addition products **7**−**9** are unstable; all of them may undergo C−N cleavage, and C−X cleavage might be an alternative option for **8** and **9**. The C−N cleavage is a retro-ene reaction to the δ-oxoalkyl diazotic acids **10**−**12**, which lead to DNA-alkylating diazonium ions.[10] For **8** and **9**, C−X cleavage might be possible in condensed phase by way of water-assisted C−X cleavage, and we are studying this process using the reactions of the microsolvated models **13** and **14** to the *N*-nitrosoamides **15** and **16**, respectively, which also undergo thermal decomposition to DNA-alkylating diazonium ions.[11] We focus on the comparative analysis of C−N versus C−X cleavages, and the analysis is somewhat complex because **7**−**9** occur in several conformations of rotamers. We will show that the NN-isomerization barriers are comparable to the barriers for the ring-opening reactions. It is for this reason that two Curtin−Hammett scenarios[12] need to be studied: one for the NN-*trans*-rotamers of **7**−**9** to undergo C−X cleavage or NN-isomerization and another one for the NN-*cis*-rotamers to undergo C−X cleavage, C−N cleavage, or NN-isomerization. Thus, comparisons of the energies of the competing reaction and isomerization transition states are required. We performed complete searches for the conformers of **7**−**16** to ensure that we considered all possibly relevant transition state structures, and the discussion will focus on the reaction and isomerization transition states.

Computational Methods

Hybrid density functional theory was employed.[13,14] The B3LYP method[15,16] is widely used and considered highly accurate.[17,18] All calculations employed the 6-31G** basis set.[19] In our previous study of **4**, we reported energies computed using full fourth-order perturbation theory, and that study may serve as a calibration.[7] In general, all relevant stationary structures were located with gradient methods[20] and vibration analyses were carried out to confirm and characterize the stationary structure and to obtain thermochemical information.[21] Calculations were carried out with Gaussian03[22] and earlier versions.

(3) (a) Yang, C. S.; Smith, T. J. *Adv. Exp. Med. Biol.* **1996**, *387*, 385. (b) Yang, C. S.; Tu, Y. Y.; Koop, D. R.; Coon, M. J *Cancer Res.* **1985**, *45*, 1140. (c) *Chemical Carcinogens*; Preusmann, R., Stewart, B. W., Searle, C. E., Eds.; ACS Monograph 1984; American Chemical Society: Washington, DC, 1984; p 643. (d) Mochizuki, M.; Anjo, T.; Okada, M. *Tetrahedron Lett.* **1980**, *21*, 3693.

(4) (a) Mesic, M.; Peuralahti, J.; Blans, P.; Fishbein, J. C. *Chem. Res. Toxicol*. **2000**, *13*, 983. (b) Cai, H.; Fishbein, J. C. *J. Am. Chem. Soc*. **1999**, *121*, 1826. (c) Chahoua, L.; Mesic, M.; Revis, C. L.; Vigroux, A.; Fishbein, J. C. *J. Org. Chem.* **1997**, *62*, 2500. (d) Revis, C. L.; Rajamaki, M.; Fishbein, J. C. *J. Org. Chem.* **1995**, *60*, 7733. (e) Reynolds, C. A.; Thomson, C. *J. Chem. Soc., Perkin Trans. 2* **1987**, 1337.

(5) Wong, H. L.; Murphy, S. E.; Hecht, S. S. *Chem. Res. Toxicol*. **2005**, *18*, 61.

(6) (a) Chahoua, L.; Cai, H.; Fishbein, J. C. *J. Am. Chem. Soc.* **1999**, *121*, 5161. (b) Chahoua, L.; Vigroux, A.; Chiang, Y.; Fishbein, J. C. *Can. J. Chem.* **1999**, *77*, 1148.

(7) Glaser, R. *J. Am. Chem. Soc.* **1999**, *121*, 5170.

(8) Loeppky, R. N.; Yu, H. *J. Org. Chem.* **2004**, *69*, 3015.

(9) (a) Rajadhyaksha, V. J. PCT Int. Appl., 1988, 63. (b) Laubie, M.; Poignant, J. C.; Scuvee-Moreau, J.; Dabire, H.; Dresse, A.; Schmitt, H. *J. Pharmacol.* **1985**, *16*, 259.

(10) (a) Moss, R. A.; Lane, S. M. *J. Am. Chem. Soc.* **1967**, *89*, 5655. (b) Moss, R. A. *J. Org. Chem.* **1966**, *31*, 1082.

(11) (a) White, E. H. *Organic Synthesis*; Wiley: New York, 1973. (b) White, E. H.; Dzadzic, P. M. *J. Am. Chem. Soc.* **1976**, *98*, 4020. (c) White, E. H.; Elliger, C. A. *J. Am. Chem. Soc.* **1967**, *89*, 165. (d) White, E. H. *J. Am. Chem. Soc.* **1955**, *77*, 6014. (e) White, E. H. *J. Am. Chem. Soc.* **1955**, *77*, 6011 and references therein.

(12) (a) Seeman, J. I. *Chem. Rev.* **1983**, *83*, 83. (b) Curtin, D. Y. *Rec. Chem. Prog.* **1954**, *15*, 111.

(13) Koch, W.; Holthausen, M. C. *A Chemist's Guide to Density Functional Theory*; Wiley-VCH: Weinheim, 2000.

(14) (a) Kohn, W.; Sham, L. J. *Phys. Rev. A* **1965**, *140*, 1133. (b) Hohenberg, P.; Kohn, W. *Phys. Rev. B* **1964**, *136*, 864.

(15) Becke, A. D. *J. Chem. Phys.* **1993**, *98*, 5648.

(16) (a) Miehlich, B.; Savin, A.; Stoll, H.; Preuss, H. *Chem. Phys. Lett.* **1989**, *157*, 200. (b) Lee, C.; Yang, W.; Parr, R. G. *Phys. Rev. B* **1988**, *37*, 785.

(17) (a) Becke, A. D. *J. Chem. Phys*. **1993**, *98*, 5648. (b) Hohenberg, P.; Kohn, W. *Phys. Rev. B* **1964**, *136*, 864. (c) Kohn, W.; Sham, L. J. *Phys. Rev. A* **1965**, *140*, 1133.

(18) (a) Raghavachari, K. *Theor. Chem. Acc.* **2000**, *103*, 361. (b) Curtiss, L. A.; Raghavachari, K.; Redfern, P. C.; Pople, J. A. *J. Chem. Phys.* **1997**, *106*, 1063. (c) Clark, D. L.; Hobart, D. E.; Neu, M. P. *Chem. Rev.* **1995**, *95*, 25.

(19) (a) Francl, M. M.; Pietro, W. J.; Hehre, W. J.; Binkley, J. S.; Gordon, M. S.; DeFrees, D. J.; Pople, J. A. *J. Chem. Phys*. **1982**, *77*, 3654. (b) Hariharan, P. C.; Pople, J. A. *Chem. Phys. Lett.* **1977**, *51*, 192. (c) Hariharan, P. C.; Pople, J. A. *Theor. Chim. Acta* **1973**, *28*, 213. (d) Pople, J.; Beveridge, D.; Dobosh, P. *J. Am. Chem. Soc*. **1968**, *90*, 4201.

(20) Peng, C.; Ayala, P. Y.; Schlegel, H. B.; Frisch, M. J. *J. Comput. Chem*. **1996**, *17*, 49.

(21) McQuarrie, D. A.; Simon, J. D. *Molecular Thermodynamics*; University Science Books: Sausalito, CA, 1999.

All computed structural data are documented in Supporting Information, and we show models only of the most relevant conformations of the substrates and products of the ring-opening reactions and of the transition state structure between them (Figures 1, 2, and 4). Total energies E (in atomic units), vibrational zero-point energies $VZPE$ (kcal·mol^{-1}), thermal energies TE (kcal·mol^{-1}, 298.15 K), and entropies S (cal·mol^{-1}·K^{-1}) are reported as part of Supporting Information. With these data, we computed values for ΔE, $\Delta E_0 = \Delta E + \Delta VZPE$, $\Delta H_{298} = \Delta E + \Delta TE + \Delta RT$, and $\Delta G_{298} = \Delta H_{298} - 0.29815\Delta S$, and we report and discuss ΔG_{298} data unless noted otherwise. To allow for direct comparison, most data are provided in Table 1. Throughout this paper, bond lengths are given in angstroms, bond angles in degrees, and relative and reaction energies in kcal·mol^{-1}.

Results and Discussion

Cyclic Imines, *N*-Nitrosoiminium Ions, and α-Hydroxy-*N*-Nitrosamines. Structures of Δ^1-pyrroline **1**, 2-imidazoline **2**, and 2-oxazoline **3** are unremarkable except for their pucker. Whereas **1** and **2** are puckered, imine **3** is totally flat. The pucker in **1** and **2** moves the methylene group out of the plane, and for **2**, the amine pyramidalization places the H-atom on the same side as the methylene group. We are interested in the products of HONO addition to **1**−**3**, the α-hydroxy-*N*-nitrosamines **7**−**9**. This addition most likely proceeds by acid catalysis to generate NO$^+$,[23] regioselective electrophilic addition of NO$^+$ to the imine to form *N*-nitrosoiminium ions **4**−**6**, and subsequent water addition and deprotonation. The ions **4**−**6** are of interest in their own right because they are thought to be the reactive species in acid-catalyzed conversion of α-acetoxy-*N*-nitrosamines to the respective alcohols.[6,7]

Cis and *trans* N-N-rotamers were considered for **4**−**6** as well as the transition state structures TS-**4**−TS-**6** for rotational isomerization (Scheme 2). The *trans*-ions are preferred and N−N rotations are fast with activation barriers (NN-*s-cis* → TS) below 10 kcal·mol^{-1} (Table 1) and some 10−15 kcal·mol^{-1} lower than in the corresponding neutral *N*-nitrosamines (vide infra). The thermodynamic *trans*-preference is important because it results in a kinetic *trans*-preference for the formation of α-hydroxy-nitrosamines **7**−**9**. On the basis of the ΔG values of Table 1, alcohols **7**−**9** are formed over 90% as the *trans*-isomer; the exp(−$\Delta G/RT$) values are 93%:7%, 99%:1%, 98%:2%, respectively.

The α-hydroxy-*N*-nitrosamines **7**−**9** give rise to a large number of possible conformations. Again NN-*s-cis* and *-s-trans* conformations are possible, and Scheme 3 illustrates the additional options due to ring puckering and O−H bond orientation. In the **a**-structures, the OH and CH_2 groups are on the same side of the ring and vice versa for the **b**-structures. For **8**, there is an additional option related to the direction of the N-pyramidalization. The N−H bond is equatorial or axial in the unprimed and primed structures, respectively. Possible orientations of O−H bond may lead to three staggered conformations designated as NO, IN, and X. In the NO structures, the O−H bond is on the same side of the N=O group; in the

TABLE 1. Comparison of Pertinent Relative and Reaction Energies for Various X (CH_2, NH, O)

parameter[a]	X = CH_2	X = NH	X = O
	4	**5**	**6**
$G_{trans-\text{pref}}$	1.50	2.71	2.16
G_A(NN-*cis* to TS)	3.57	7.40	4.22
G_A(NN-*trans* to TS)	5.07	10.11	6.38
	7	**8**	**9**
G_{react}(HONO + imines)	−10.80	−4.63	−3.39
G_A(NO-*cis* to TS)		18.95	27.51
G_A(NO-*trans* to TS)		19.31	27.67
G_A(X-*cis* to TS)		21.03	19.82
G_A(X-*trans* to TS)		23.31	21.95
	10	**11**	**12**
G_{rel}(**a** vs **d**)	0.10	0.92	0.96
G_{rel}(**b** vs **d**)	0.59	1.10	4.31
G_{rel}(**c** vs **d**)	0.11	1.50	4.29
G_{react}(NO-*cis*-%**a** → #**a**)	4.32	−15.78	−12.32
G_{react}(NO-*cis*-%**b** → #**b**)	4.99	−15.60	−10.10
G_{react}(NO-*cis*-**8a′** → **11a**)		−15.31	
G_{react}(NO-*cis*-**8b′** → **11b**)		−14.30	
G_A(NO-*cis*-%**a** → #**a**)	20.84	20.72	16.44
G_A(NO-*cis*-%**b** → #**b**)	20.26	19.54	14.58
G_A(NO-*cis*-**8a′** → **11a**)		14.76	
G_A(NO-*cis*-**8b′** → **11b**)		12.14	
		13	**14**
$G_{exo-\text{pref}}$(*trans*)		0.26	−0.13
$G_{exo-\text{pref}}$(cis)		0.16	−0.17
G_{ms}(*exo-trans-*%)		−1.06	−0.28
G_{ms}(*endo-trans-*%)		−0.79	−0.42
G_{ms}(*exo-cis-*%)		−0.79	−0.09
G_{ms}(*endo*-cis-%)		−0.63	−0.08
		15	**16**
G_{react}(X-*trans-*% → #)		−10.00	−8.91
G_{react}(X-*cis-*% → #)		−12.28	−11.04
G_A(*exo-trans-*% → #)		17.26	21.29
G_A(*endo-trans-*% → #)		16.73	23.08
G_A(*exo-cis-*% → #)		17.24	20.62
G_A(*endo-cis-*% → #)		16.49	19.85
		TS(**13**,**15**)	TS(**14**,**16**)
$G_{exo-\text{pref}}$(*trans*)		−0.27	1.66
$G_{exo-\text{pref}}$(cis)		−0.58	−0.94

[a] Symbols % and # are used as wildcard characters.

SCHEME 2. Conformations for *N*-Nitrosoiminium Ions 4−6

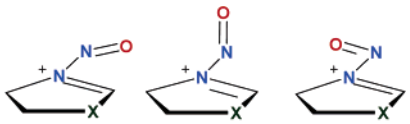

X = CH_2	NN-*cis* **4**	TS-**4**	NN-*trans* **4**
X = NH	NN-*cis* **5**	TS-**5**	NN-*trans* **5**
X = O	NN-*cis* **6**	TS-**6**	NN-*trans* **6**

(22) Frisch, M. J.; Trucks, G. W.; Schlegel, H. B.; Scuseria, G. E.; Robb, M. A.; Cheeseman, J. R.; Montgomery, J. A., Jr.; Vreven, T.; Kudin, K. N.; Burant, J. C.; Millam, J. M.; Iyengar, S. S.; Tomasi, J.; Barone, V.; Mennucci, B.; Cossi, M.; Scalmani, G.; Rega, N.; Petersson, G. A.; Nakatsuji, H.; Hada, M.; Ehara, M.; Toyota, K.; Fukuda, R.; Hasegawa, J.; Ishida, M.; Nakajima, T.; Honda, Y.; Kitao, O.; Nakai, H.; Klene, M.; Li, X.; Knox, J. E.; Hratchian, H. P.; Cross, J. B.; Bakken, V.; Adamo, C.; Jaramillo, J.; Gomperts, R.; Stratmann, R. E.; Yazyev, O.; Austin, A. J.; Cammi, R.; Pomelli, C.; Ochterski, J. W.; Ayala, P. Y.; Morokuma, K.; Voth, G. A.; Salvador, P.; Dannenberg, J. J.; Zakrzewski, V. G.; Dapprich, S.; Daniels, A. D.; Strain, M. C.; Farkas, O.; Malick, D. K.; Rabuck, A. D.; Raghavachari, K.; Foresman, J. B.; Ortiz, J. V.; Cui, Q.; Baboul, A. G.; Clifford, S.; Cioslowski, J.; Stefanov, B. B.; Liu, G.; Liashenko, A.; Piskorz, P.; Komaromi, I.; Martin, R. L.; Fox, D. J.; Keith, T.; Al-Laham, M. A.; Peng, C. Y.; Nanayakkara, A.; Challacombe, M.; Gill, P. M. W.; Johnson, B.; Chen, W.; Wong, M. W.; Gonzalez, C.; Pople, J. A. *Gaussian 03*, Revision C.02; Gaussian, Inc.: Wallingford CT, 2004.

(23) Wu, H.; Glaser, R. *J. Phys. Chem. A* **2003**, *107*, 11112.

SCHEME 3. Possible Conformations of α-Hydroxynitrosamines 7−9

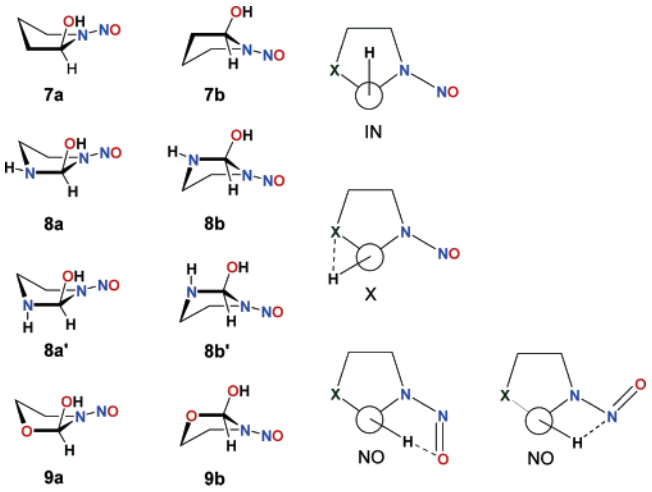

TABLE 2. Relative Energies (ΔG_{rel}) of *trans*- and *cis*-α-Hydroxy-*N*-nitrosamines 7−9[a]

molecule		*trans* IN	*trans* X	*trans* NO	*cis* IN	*cis* X	*cis* NO
7	**a**	2.25	2.76	0.00	4.58	–	0.18
	b	–	–	1.07	–	–	0.00
8	**a**	1.46	–	0.00	3.75		0.00
	a′	2.05	1.52	2.02	4.34	3.44	1.58
	b	–	–	–	–	–	0.74
	b′	–	–	2.65	–	–	2.05
9	**a**	0.38	0.00	0.60	–	1.37	0.00
	b	0.11	–	–	1.57	–	1.13

[a] Potential conformers that do not exist on the PES are marked by "–".

IN structures, O−H bond is directed toward the inside of the ring; and in the X structures, it is projected toward the X-group. Consequently, 12 conformations might exist for **7** and **9**, and 24 conformations are possible for **8**. Of these possible structures, our calculation show the existence of seven structures of **7**, 13 structures of **8**, and eight structures of **9**.

Table 2 shows the relative energies of the existing IN, X, and NO conformers for the *trans*- and *cis*-isomer of α-hydroxy-*N*-nitrosamines relative to the most stable structure of the same N-N-rotamer. The NN-*cis*-structures NO-**7b** ≈ NO-**7a**, NO-**8a**, and NO-**9a** are the most stable *cis*-structures, and this can be attributed to intramolecular OH···ON hydrogen bonding (NO-**7b** and NO-**7a** 2.157 Å, NO-**8a** 2.164 Å, NO-**9a** 2.120 Å). The planarity of the ring N-atom shows its sp^2 hybridization and suggests the involvement of its lone pair in $>N^+=N-O^-$ delocalization that enhances the acceptor ability of the nitroso−O atom (Scheme 3, right). The NN-*trans*-structures can only realize rather long, nonlinear, and weak OH···NO hydrogen bonding in a five-membered ring. With this disadvantage for the NO conformation, the alternative of an intramolecular X···HO hydrogen bond becomes more competitive, and for X = O, the latter even wins: the structures NO-**7a**, NO-**8a**, and X-**9a** are the most stable *trans*-structures (NO-**7a** 2.961 Å, NO-**8a** 3.005 Å, X-**9a** 2.545 Å, NO-**9a** 3.140 Å). The ΔG_{rel} values for the NN-*cis*-structures are less than 5 kcal·mol^{-1} and less than 3 kcal·mol^{-1} for the NN-*trans*-structures. This difference of about 2 kcal·mol^{-1} reflects the effectiveness of the OH···ON hydrogen bonding in a six-membered ring.

TABLE 3. *trans*-Preference Energies of α-Hydroxy-*N*-nitrosamines 7−9

	molecule		IN	X	NO	global	
ΔE_{pref}	**7**	**a**	2.46	–	−0.51	NO-*trans*-**7a** vs NO-*cis*-**7b**	−0.66
		b	–	–	−1.84		
	8	**a**	2.48	–	−0.83	NO-*trans*-**8a** vs NO-*cis*-**8a**	−0.83
		a′	2.35	2.39	−1.01		
		b	–	–	–		
		b′	–	–	−1.28		
	9	**a**	–	2.22	−0.83	X-*trans*-**9a** vs NO-*cis*-**9a**	0.08
		b	1.93	–	–		
ΔG_{pref}	**7**	**a**	2.45	–	0.31	NO-*trans*-**7a** vs NO-*cis*-**7b**	0.12
		b	–	–	−0.95		
	8	**a**	2.65	–	0.35	NO-*trans*-**8a** vs NO-*cis*-**8a**	0.35
		a′	2.64	2.27	−0.09		
		b	–	–	–		
		b′	–	–	−0.25		
	9	**a**	–	2.13	0.16	X-*trans*-**9a** vs NO-*cis*-**9a**	0.76
		b	2.22	–	–		

Table 3 shows the *trans*-preference energies of **7**−**9**. For the IN- and X-conformations, all ΔE_{pref} and ΔG_{pref} values are positive, there is hardly any difference between each pair of ΔE_{pref} and ΔG_{pref} values, and we take the intrinsic N−N *trans*-preference to be 2 ± 0.5 kcal·mol^{-1}. Hydrogen-bonding in the NO-structures changes the *trans*-preferences and ΔE_{pref} and ΔG_{pref} differ. The ΔE_{pref} values all are negative, that is, OH···ON and OH···NO hydrogen bonding dominates any intrinsic N−N *trans*-preference. However, not all ΔG_{pref} values are negative, and **7a**, **8a**, and **9a** prefer NN-*trans*-structures. For each pair, ΔG_{pref} is just about 1 kcal·mol^{-1} less negative than the respective ΔE_{pref}. The transferable quantity $\Delta G_{pref} - \Delta E_{pref} \approx 1$ kcal·mol^{-1} reflects the entropic disadvantage for the formation of the OH···ON bonded six-membered ring in the *cis*-structures as compared to the formation of the OH···NO hydrogen-bonded five-membered ring in the *trans*-structures.

The relative energies in columns NO, X, and IN of Table 3 measure the *trans*-preference between structures that are otherwise similar. However, Table 2 shows that the best *cis* and the best *trans*-structures might have different conformations about the C−O bond and different ring pucker. Therefore, in column "Global" in Table 3 are provided the *trans*-preference energies between the most stable *trans*- and *cis*-structure, and these ΔG data give equlilibrium *trans*:*cis* ratios of 64%:36% and 78%:22% for **8** and **9**, respectively.

***cis/trans*-Isomerization of α-Hydroxy-*N*-nitrosamines.** The N−N bond rotations in *N*-nitrosamines are restricted because of the partial double bond character ($>N^+=N-O^-$). The activation barriers usually fall in the range of 23−25 kcal·mol^{-1} and some special cases with $\Delta G^{\ddagger}$ values as low as 12−15 kcal·mol^{-1} were reported.[24] Most relevant to the present work is the study by Haky et al. of the hindered rotations in the *N*-nitroso derivatives of **1** ($\Delta G^{\ddagger}$ = 22.3 kcal·mol^{-1}) and **3** ($\Delta G^{\ddagger}$ = 18.7

(24) Polonski, T.; Pham, M.; Milewska, M. J. *J. Org. Chem.* **1996**, *61*, 3766 and references therein.

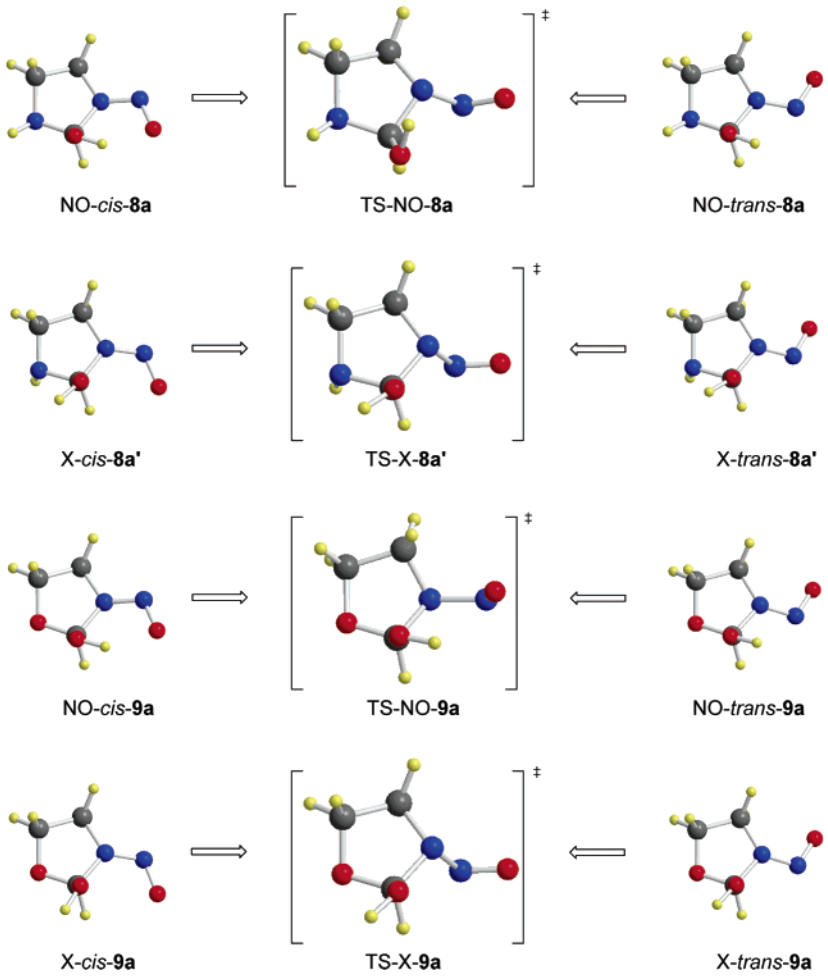

FIGURE 1. NN rotational isomerization of α-hydroxy-*N*-nitrosamines **8** and **9**.

kcal·mol^{-1}).[25] It is clear that any such barriers can be overcome at room temperature and any *trans*-**7** has to convert to *cis*-**7** prior to C−N cleavage by retro-ene reaction. No knowledge of the precise activation barrier is needed in this case because *trans*-**7** does not have any other reaction channel available. The situation is more interesting for **8** and **9**; there is the possibility for C−X cleavage and whether it is realized depends on its competition with NN isomerization and C−N cleavage in the *cis*-rotamer. We located the transition state structures for two paths for **8** and **9** (Figure 1). A priori any pair of conformers of a NN-*cis*- and a NN-*trans*-rotamer could be connected by an isomerization path and we make the reasonable assumption that the OH orientation is retained during the NN isomerization. The orientation was in fact retained for three of the four paths. Searching for the transition state structure and starting with NO-*trans*-**8a**, resulted in the IN-transition state shown in Figure 1. We explored both directions for NN-rotation and report only the favorable one. The activation energies are provided in Table 1; they are in the "normal" range and they are somewhat high for NO-**9**.

Thermodynamics of α-Hydroxy-*N*-nitrosamines Formation. The addition of water and alcohols to carbonyls are equilibria that lead to the formation of hydrates and acetals and for some aldehydes the equilibria lie on the adduct side.[26] Imines react by addition/elimination to carbonyls.[27,28] The related acid-catalyzed addition of RO−NO to carbonyls apparently has not been reported.[29] The known α-alkoxy-*N*-nitrosamines formally are the products of RO−NO addition to imines, but their actual formation is more involved.[30] The ON−Cl addition to imines was demonstrated by Wiessler et al.,[31] and the resulting α-chloro-*N*-nitrosamines readily react with acetates to α-acetoxy-*N*-nitrosamines. The additions of HNO_2 to the cyclic imines **1**−**3** all are exothermic, and moreover, their exothermicities are so high as to over-

(25) Haky, J. E.; Saavedra, J. E.; Hilton, B. D. *Org. Magn. Res.* **1983**, *21*, 79.

(26) (a) Wiberg, K. B.; Morgan, K. M.; Maltz, H. *J. Am. Chem. Soc.* **1994**, *116*, 11067. (b) Bell, R. P. *Adv. Phys. Org. Chem.* **1966**, *4*, 1.

(27) (a) Novak, M.; Helmick, J. S.; Oberlies, N.; Rangappa, K. S.; Clark, W. M.; Swenton, J. S. *J. Org. Chem.* **1993**, *58*, 867. (b) Ishino, R.; Kumanotani, J. *J. Org. Chem.* **1974**, *39*, 108. (c) Koehler, K.; Sandstrom, W.; Cordes, E. H. *J. Am. Chem. Soc.* **1964**, *86*, 2413.

(28) (a) Sayer, J. M.; Conlon, P. *J. Am. Chem. Soc.* **1980**, *102*, 3592. (b) Hine, J.; Craig, L. C.; Underwood, J. G., Jr.; Via, F. A. *J. Am. Chem. Soc.* **1970**, *92*, 5194.

(29) Note that the base-catalyzed RONO addition to carbonyls gives other products, the hydroxyimino compounds R-C(=O)-C(=NOH)-R′; see: Niiya, T.; Ikeda, H.; Yukawa, M.; Goto, Y. *Chem. Phar. Bull.* **2001**, *49*, 473.

(30) Eiter, von K.; Hebenbrock, K. F.; Kabbe, H. J. *Liebigs Ann. Chem.* **1972**, *765*, 55.

(31) Müller, E.; Kettler, R.; Wiessler, M. *Liebigs Ann. Chem.* **1984**, 1468.

SCHEME 4. Conformations of (*E*)-*δ*-Oxobutyl Diazotic Acids 10−12

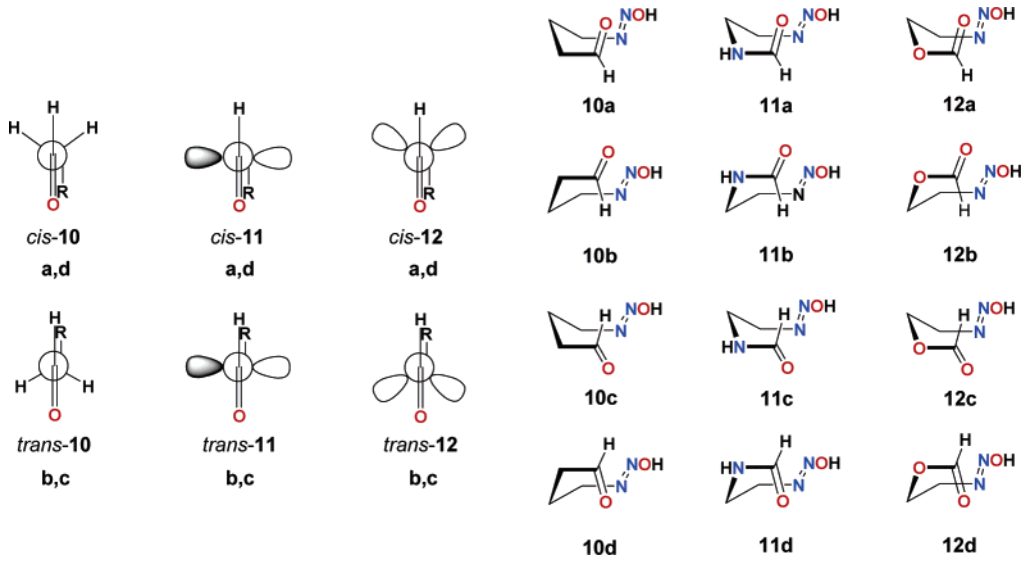

compensate for any entropy losses and the reactions also are exergonic (Table 1).

Retro-Ene C−N Cleavage Reactions. Retro-ene reactions involve an intramolecular transfer of a *γ*-hydrogen atom to an unsaturated center via a six-electron cyclic transition state.[32] These reactions formally are the reverse of well-known ene reactions.[33] The retro-ene reactions of **7**−**9** lead to the *δ*-oxobutyl diazotic acids **10**−**12**. Only NO-*cis* α-hydroxy-*N*-nitrosamines can undergo retro-ene reactions to form *E*-diazotic acids. We have shown above that NO-*cis*-**7b**, NO-*cis*-**8a**, and NO-*cis*-**9a** are the best NN-*cis*-structures, and these structures as well as the structures NO-*cis*-**7a**, NO-*cis*-**8a′**, NO-*cis*-**8b**, NO-*cis*-**8b′**, and NO-*cis*-**9b** all are candidates for C−N cleavage via retro-ene reaction.

Scheme 4 presents four stereoisomers of *δ*-oxobutyl diazotic acids; the carbonyl and hydroxydiazo groups are directed toward the same (**a** and **b**) or opposite (**c** and **d**) sides, respectively, and the ring-pucker places the methylene group on the same (**a** and **d**) or opposite (**b** and **c**) side with respect to the carbonyl group, respectively. The **a**- and **d**-structures are approximately CC-*s*-*cis* in that the carbonyl group is on the same side of alkyl group, whereas the **b**- and **c**-structures are CC-*s*-*trans*. Relative energies of the **a**-, **b**- and **c**-structures are listed in Table 1. All of the isomers exist, they are close in energy, and the dipole parallel-aligned **d**-isomers are best in all cases. The acids formed by the retro-ene reactions are **10a** and **10b**, **11a** and **11b**, and **12a** and **12b**, and those are shown in Figure 2.

Because of the Curtin−Hammett situations, we located all of the transition state structures for the retro-ene reactions of **7**−**9**; their structures are shown in Figure 2, and pertinent energy data are provided in Table 1. The retro-ene reaction of **7** to *δ*-oxobutyl diazotic acids **10** involves C−N cleavage and H migration via a six-membered ring transition state structure. The structural data indicate that the H migration precedes C−N cleavage in all cases. The analogues **8** and **9** show the same general characteristics.

In Figure 3, the reaction diagrams are shown for **7**−**9** to illustrate the effects of X on reactions energies and barriers. The red lines are the reactions diagrams for the most stable NO-*cis* stereoisomers, and if different, the additional lines are the reactions diagrams with the lowest activation barriers. The retro-ene reaction of **7** is endothermic and endergonic, whereas the reactions of **8** and **9** are exothermic and exergonic. Since all products **10**−**12** are labile and undergo further exothermic and exergonic decompositions, the overall reactions will proceed fast not only for **8** and **9** but also for **7**. Our interest focuses on the activation barriers and we find all of them to be less than 21 kcal·mol^{-1}. If the *cis*-isomers are accessible, their retro-ene reactions all would be fast, even at room temperature, and the relative rates would follow the order **7** > **8** ≈ **9**. We will discuss in Figure 6 whether the *cis*-isomers are accessible.

C−X Cleavage Reactions. Elimination reactions are fundamental processes in organic chemistry and have been discussed extensively.[34] Whenever possible, *anti*-elimination occurs via a transition state in which the departing groups (designated H and X) are *trans* to one another in a staggered conformation and allow for the most effective overlap between the developing *π* orbitals of the α- and *β*-carbons.[35] Although some subtle features of *syn*-concerted elimination remain controversial, there is general agreement that *syn*-periplanar elimination involves an E1cB-like mechanism,[36] and this reaction has the advantage of avoiding any zwitterionic intermediate. The direct elimination in **8** and **9** would require the transfer of the *β*-H to the X-leaving group via a four-membered ring transition state, and this process is not

(32) (a) Ripoll, J. L.; Vallee, Y. *Synthesis* **1993**, *7*, 659. (b) Paderes, G. D.; Jorgensen, W. L. *J. Org. Chem.* **1992**, *57*, 1904. (c) Dubac, J.; Laporterie, A. *Chem. Rev.* **1987**, *87*, 319.

(33) (a) Oppolzer, W.; Snieckus, V. *Angew. Chem., Int. Ed. Engl.* **1978**, *17*, 476. (b) Hoffmann, H. M. R. *Angew. Chem., Int. Ed. Engl.* **1969**, *8*, 556. (c) Alder, K.; Pascher, F.; Schmitz, A. *Ber.* **1943**, *76*, 27.

(34) (a) Gronert, S. *J. Am. Chem. Soc.* **1992**, *114*, 2349. (b) Bartsch, R. A.; Zavada, J. *Chem. Rev.* **1980**, *80*, 454, and references therein.

(35) Bach, R. D.; Badger, R. C.; Lang, T. J. *J. Am. Chem. Soc.* **1979**, *101*, 2845.

(36) (a) Sicher, J. *Angew. Chem., Int. Ed. Engl.* **1972**, *11*, 200. (b) Lebel, N. A. *Adv. Alicyclic Chem.* **1971**, *3*, 195. (c) Burnett, J. F. *Surv. Prog. Chem.* **1969**, *5*, 53. (d) Hughes, E. D.; Ingold, C. K.; Patel, C. S. *J. Chem. Soc.* **1933**, 526.

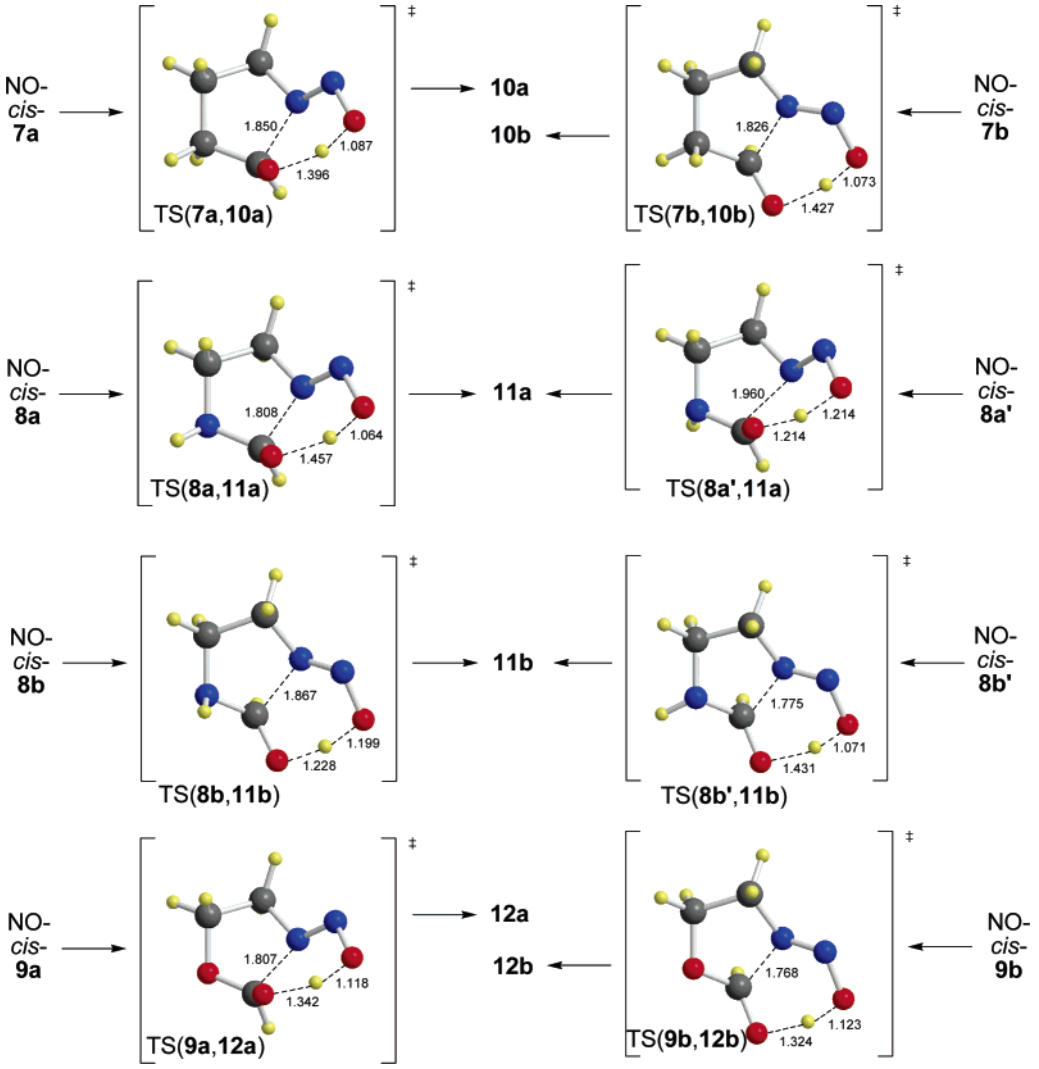

FIGURE 2. Retro-ene reactions for **7**−**9**.

likely. However, several reports in the literature demonstrate that microsolvation very effectively catalyzes this process via a six-membered ring transition state.[37−40] Hence, instead of **8** and **9**, we are considering the water adducts **13** and **14** and their reaction transition state structures to form *N*-(2-aminoethyl)- and *N*-(2-hydroxyethyl)-*N*-nitrosoformamides **15** and **16**, respectively.

The potential energy surface analysis showed that X-*trans*-**8a′** and X-*cis*-**8a′**, as well as X-*trans*-**9a** and X-*cis*-**9a**, are the conformations suited for C−X cleavage. C−X cleavage could occur equally well from any NN-*cis*- or NN-*trans*-structure, and X-conformations are easily accessible for each geometrical isomer. The structures **13** and **14**, respectively, resulting by microsolvation of X-*trans*-**8a′** and X-*cis*-**8a′** and of X-*trans*-**9a** and X-*cis*-**9a**, respectively, are shown in Figure 4. The *endo* and *exo* conformations of **13** and **14** differ in the orientation of lone pairs on the O-atom of the water molecule. Solvation energy data are given in Table 1, and *exo* and *endo* microsolvation is almost isoenergetic. Two hydrogen bonds result in solvation energies ΔE of 11−13 kcal·mol^{-1}, whereas the ΔG values are close to zero because of loss of the entropy associated with the hydrate formation. Hence, microsolvated substrates are accessible in *some* concentration, and that is the only issue that matters.

The C−X cleavage leads to *N*-(2-aminoethyl)- and *N*-(2-hydroxyethyl)-*N*-nitroso-formamides **15** and **16** and the *N*-nitroso-formamides can assume a variety of conformations (Scheme 5). *N*-Nitrosoformamides can form *E*/*Z*-isomers about the NN and NC bonds. Some of these are less likely than others—the (NN-*Z*, CN-*Z*) isomer, for example, suffers greatly from dipole alignment and lone pair repulsion—and the (NN-*E*, CN-*E*) isomer is best for the parent system.[41] We examined exclusively (NN-*E*, CN-*E*) structures and we focused attention instead on the possible conformations about the C−C−X bonds at

(37) Li, W.; McKee, M. L. *J. Phys. Chem. A* **1997**, *101*, 9778.
(38) (a) Lewis, M.; Glaser, R. *Chem. Eur. J.* **2002**, *8*, 1934. (b) Lewis, M.; Glaser, R. *J. Am. Chem. Soc.* **1998**, *120*, 8541.
(39) Lewis, M.; Glaser, R. *J. Phys. Chem. A* **2003**, *107*, 6814.
(40) (a) Allen, A. D.; Fedorov, A. V.; Tidwell, T. T.; Vukovic, S. *J. Am. Chem. Soc.* **2004**, *126*, 15777. (b) Chiang, Y.; Jefferson, E. A.; Kresge, A. J.; Popik, V. V. *J. Am. Chem. Soc.* **1999**, *121*, 11330. (c) Andaos, J.; Chiang, Y.; Kresge, A. J.; Pojarlieff, I. G.; Schepp, N. P.; Wirz, J. *J. Am. Chem. Soc.* **1994**, *116*, 73. (d) Bothe, E.; Dessouki, A. M.; Schulte-Frohlinde, D. *J. Phys. Chem.* **1980**, *84*, 3270. (e) Bothe, E.; Meier, H.; Schulte-Frohlinde, D.; von Sonntag, C. *Angew. Chem., Int. Ed. Engl.* **1976**, *15*, 380.

(41) Birney, D. M. *Org. Lett.* **2004**, *6*, 851.

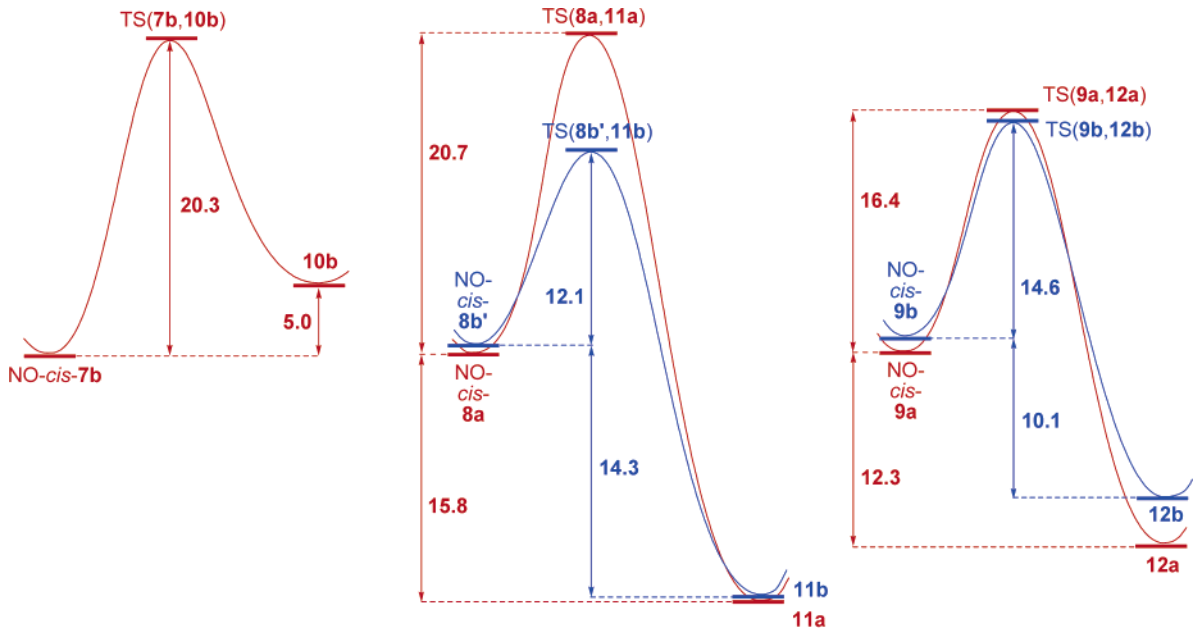

FIGURE 3. Energy (Δ*G*) diagrams for the retro-ene reactions of **7**−**9**. For **8** and **9**, the paths are shown for the reaction of the most stable substrate and for the reaction with the lowest activation barrier.

SCHEME 5. Conformations of *N*-Nitrosoformamides 15 and 16

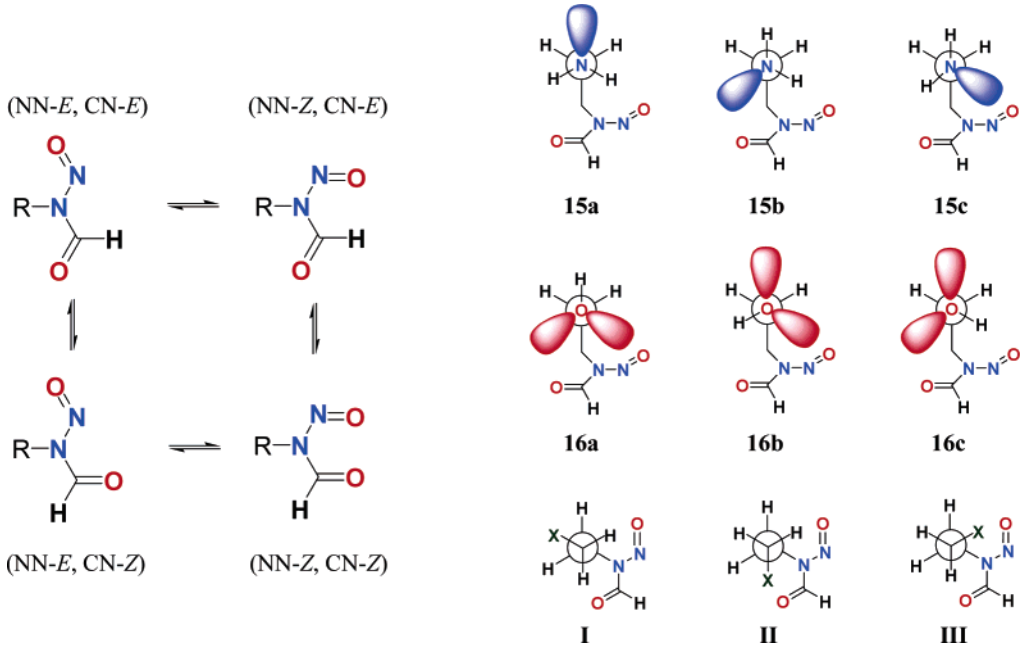

TABLE 4. Relative Stabilities (ΔG_{rel}) of Conformers of 15 and 16

	15	16
a-I	0.14	1.96
a-II	**0.00**	1.53
a-III	0.37	1.88
b-I	1.38	0.28
b-II	0.36	1.42
b-III	0.54	1.31
c-I	0.35	**0.00**
c-II	0.54	1.19
c-III	1.54	1.03

the other end of the molecule. Conformers that differ with respect to the C−X bond are designated as the **a**-, **b**-, and **c**-structures, and conformations about the C−C bond are denoted as **I**, **II** and **III**. With regard to the C−X bond conformation, the primary product requires proximity of the eliminated XH−hydrogen and the carbonyl O−atom it came from. This condition is met in all of the conformations with the only exception of the **a**-structure of **16**. The nine conformers were located for both **15** and **16** and their energies are reported in Table 4 relative to the most stable conformation.

All nine possible conformations actually exist, and this is a first indication that there are no overwhelming intramolecular stabilizations of any particular conformation and the relative energies all are small (Table 4). The **II** structures are the primary products of the cleavage reactions and will quickly convert to **I** or **III** structures.

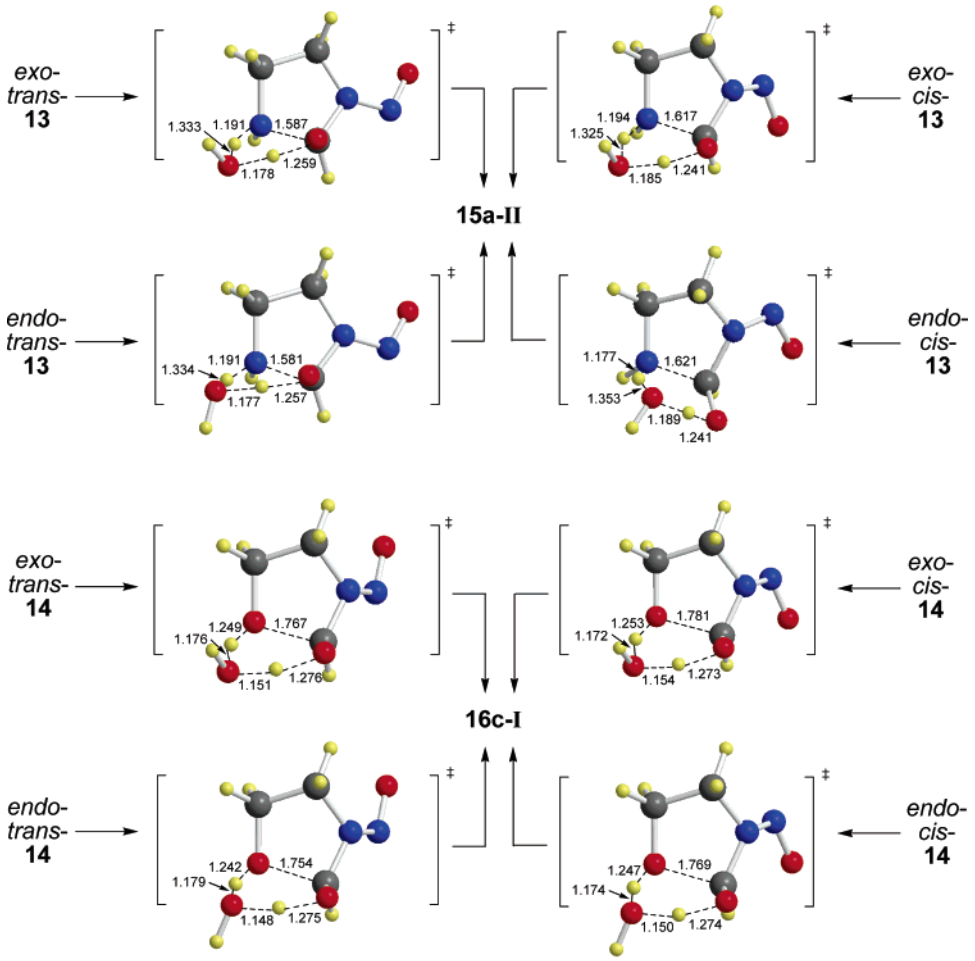

FIGURE 4. C−X cleavage reactions of microsolvated **8** and **9**.

In Figure 4, we show the most stable structures with the understanding that these figures are simplifications in that the transition state structures shown might be connected to other isomers that are in fast equilibria with the shown products.

The Curtin−Hammett situation requires the determination of all the transition state structures for the C−X cleavage reactions of **13** and **14**. Eight six-membered ring transition state structures for the reactions of **13** or **14** to products **15** or **16**, respectively, were located (Figure 4). The alcohol(O)···H···O(water) and water(O)···H···X hydrogen bonds are markedly unsymmetrical. For X = NH, both H-transfers are early and the H-transfer from water to NH is most advanced. For X = O on the other hand, only the H-transfer from the alcohol to the water is early.

In Figure 5, the reaction diagrams are shown for **8** and **9** to illustrate the effects of X on reactions energies and barriers. The red lines are the reaction diagrams for the most stable X-stereoisomers, and the brown and green lines, respectively, are the reactions diagrams for the reactions with the lowest activation barriers. The C−N cleavage reactions both are exothermic and exergonic (Table 1). Since we considered exclusively (NN-*E*, CN-*E*) products, the reactions energies might be slightly more negative. There is hardly any effect of X on the reaction energies, and the reaction exothermicities are just about 7.5 kcal·mol^{-1} and the exergonicities both are very close to 9.5 kcal·mol^{-1}. Since the products **15** and **16** are labile *N*-nitrosoamides, the overall reactions will proceed irreversibly.

Our interest focuses on the activation barriers. We find all of them to be less than 23 kcal·mol^{-1} (Table 1), and they can be as low as 16.5 kcal·mol^{-1} for X = NH and 19.9 kcal·mol^{-1} for X = O. These reactions all would be fast, even at room temperature, and whether they occur depends on the competition with the retro-ene reaction.

Curtin−Hammett Analysis. The discussion of all of the vital components of the α-hydroxy-nitrosamine decomposition scenarios now allows for the emergence of the bigger picture (Figure 6). Curtin−Hammett scenario **I** applies to the NN-*trans* α-hydroxynitrosamine undergoing C−X cleavage or NN-isomerization (yellow background) and Curtin−Hammett scenario **II** applies to the NN-*cis* α-hydroxynitrosamine undergoing C−N cleavage, or C−X cleavage, or NN-isomerization (green background). The interconversions between **8** and **13** and between **9** and **14** are facile (vide supra) and straight lines are shown for simplicity. The NN-*cis* isomers can undergo C−N and C−X cleavage and both options are indicated in **II**.

The imine **2** (X = NH) is converted to **8** and **8** is formed mostly as the NN-*trans* isomer. *trans*-**8** may undergo C−N_{amine} cleavage via its microsolvated adduct **13** (left in Figure 6) or it may isomerize to *cis*-**8**. The partitioning

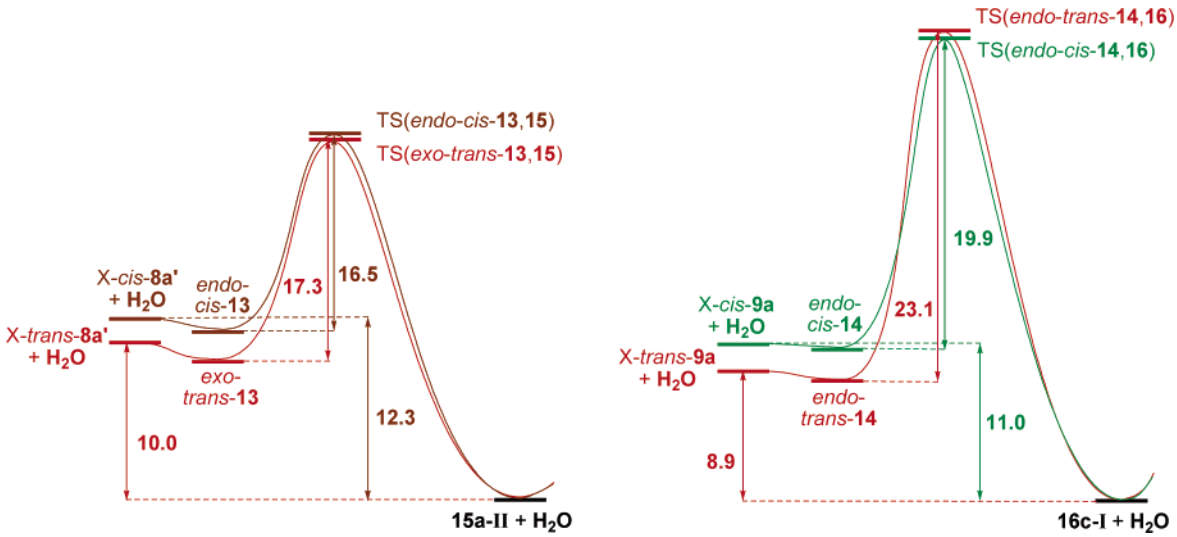

FIGURE 5. Energy (ΔG) diagrams of the C−X cleavage reactions of **8** and **9**.

between the reaction channels is determined by the relative energy of the lowest transition state structures along those two paths. Figure 6 shows that the *endo-trans* TS(**13**,**15**) is preferred over TS-NO-**8a** by $\Delta\Delta G^{\ddagger} = 1.9$ kcal·mol^{-1}; this energy difference indicates a 96%:4% preference for C−X cleavage of the NN-*trans* alcohol. Nitrosoformamide formation, a process entirely impossible in the gas-phase, now emerges as a viable option in condensed phase because of the catalysis provided by microsolvation. The small amount of NN-*trans* alcohol that is converted into the NN-*cis* isomer will immediately and exclusively undergo C−N cleavage via retro-ene reaction; TS(**8b′**,**11b**) is preferred over TS-NO-**8a** by $\Delta\Delta G^{\ddagger} = 6.1$ kcal·mol^{-1} and over *endo-cis* TS(**13**,**15**) by $\Delta\Delta G^{\ddagger} = 6.5$ kcal·mol^{-1}. The computational analysis suggests that C−N_{amine} cleavage product is not formed from the NN-*cis* alcohol. Any and all initially formed NN-*cis* alcohol is predicted to undergo retro-ene reaction.

Combining the 96%:4% preference for C−N_{amine} cleavage of the NN-*trans* alcohol with the 99%:1% advantage for the *kinetic* formation of the *trans*-alcohol, the theoretical model predicts 95% product from C−N_{amine} cleavage. Assuming error bars of ±1 kcal·mol^{-1} for $\Delta\Delta G^{\ddagger}$, the data still suggest that C−N_{amine} cleavage dominates and causes 81−98% of products. Combining the 96%:4% preference for C−N_{amine} cleavage of the NN-*trans* alcohol with the 64%:36% advantage for the *thermodynamic* formation of the *trans*-alcohol, the model predicts 62% product from C−N_{amine} cleavage, and with the error bars above, the prediction falls in the range of 53−64%.

The imine **3** (X = O) is converted to **9** and **9** is formed mostly as the NN-*trans* isomer. *trans*-**9** may undergo C−O cleavage via its microsolvated adduct **14** (left in Figure 6), or it may isomerize to *cis*-**9**. In contrast to the case of X = NH, for X = O the NN-isomerization via TS-X-**9a** is preferred over the C−O cleavage reaction via the *endo-trans* TS(**14**,**16**) by $\Delta\Delta G^{\ddagger} = 0.7$ kcal·mol^{-1}. Hence, in the Curtin−Hammett scenario **I** both options are competitive and the theoretical analysis suggests a 77%:23% advantage for isomerization. The Curtin−Hammett scenario **II** is qualitatively the same for imidazoline **2** and 2-oxazoline **3**. The transition state structure TS-(**9b**,**12b**) for retro-ene reaction is greatly preferred over the transition state structure TS-X-**9a** for NN-isomerization; the preference of $\Delta\Delta G^{\ddagger} = 5.5$ kcal·mol^{-1} guarantees quantitative retro-ene reaction. As with the case X = NH, *exo-cis* TS(**14**,**16**) is too high and C−O cleavage of NN-*cis* **14** is not an option.

Combining the 23%:77% preference for C−O cleavage of the NN-*trans* alcohol with the 98%:2% advantage for the *kinetic* formation of the *trans*-alcohol, the theoretical model predicts 23% product from C−O cleavage. Since $\Delta\Delta G^{\ddagger}$ is negative in the case X = O, the nature of the exponential function causes any error in the chemical accuracy to affect the predicted product yield more drastically. Hence, considering error bars of ±1 kcal·mol^{-1} for $\Delta\Delta G^{\ddagger}$, the yield of C−O cleavage products can fall in the rather wide range of 5−61%. Combining the 23%:77% preference for C−O cleavage of the NN-*trans* alcohol with the 78%:22% advantage for the *thermodynamic* formation of the *trans*-alcohol, the model predicts 18% product from C−O cleavage and, with the error bars above, the prediction falls in the range of 4−49%. At the very least, the theoretical analysis makes it clear that C−O cleavage is an option that warrants consideration in condensed phase while no such option exists in the gas phase at all.

Conclusion

A comparative analysis has been presented of the nitrosation chemistry of the imines **1**−**3** via the α-hydroxy-*N*-nitrosamines **7**−**9**. Several important insights have resulted from the mechanistic analysis and the analysis of the computed data.

For **7**, the retro-ene reaction of its NN-*cis*-isomer is the only decomposition path available and the diazotic acid **10** will be formed. In gas phase, the retro-ene reaction also is the only option for **8** and **9** because of the high activation barrier for C−X cleavage via a four-membered ring transition state structure as compared to the barrier for NN-isomerization. In contrast, it is the major conclusion of this study that water-assisted C−X cleavage provides powerful catalysis and renders C−X cleavage a viable option in condensed phase. For **8**, we thus predict the formation of diazotic acid **11** via retro-ene reaction

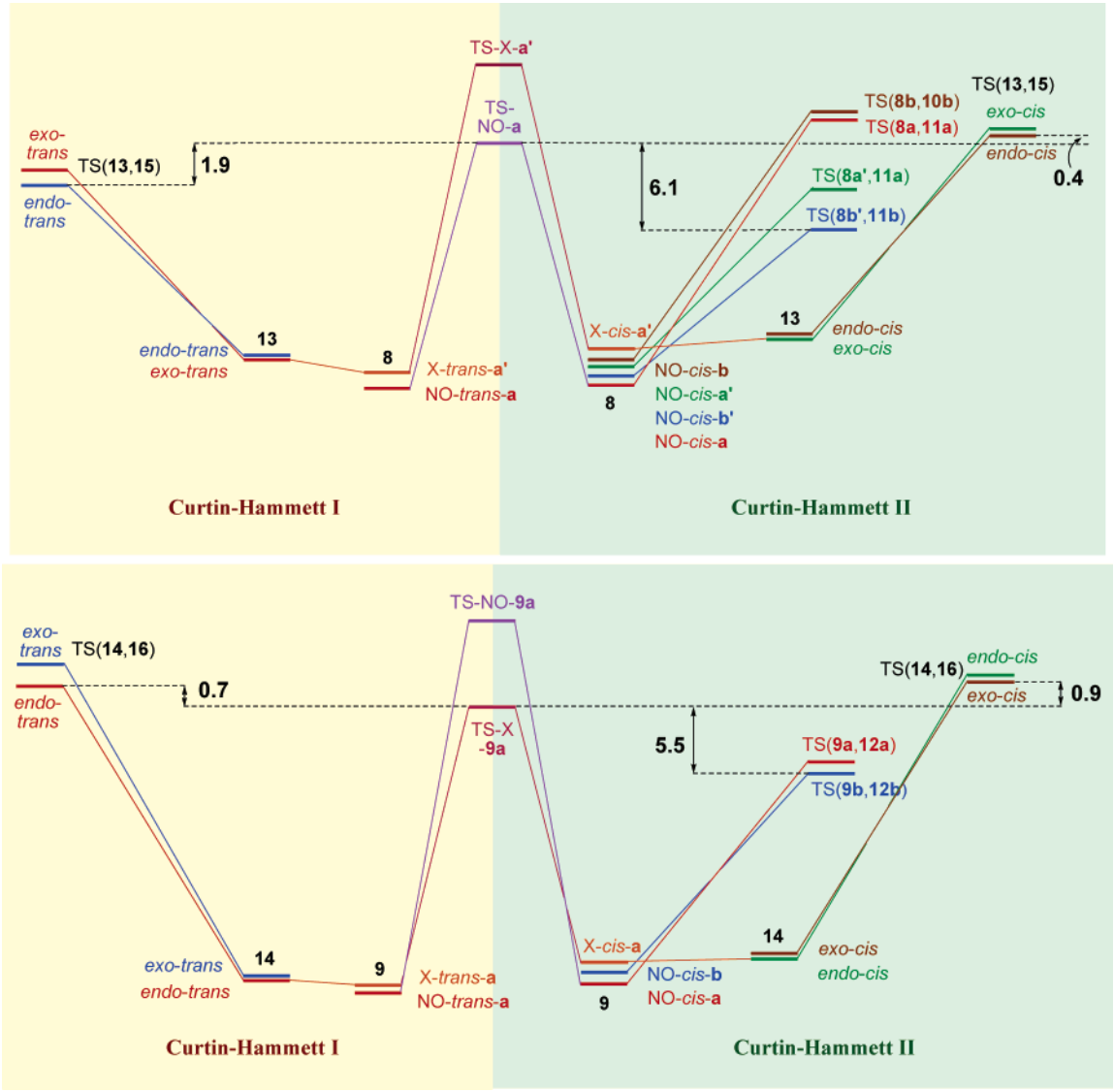

FIGURE 6. Diagrams of decomposition reactions of **8** and **9**. (No correspondence is implied by same colors in left and right half of diagram.)

and of *N*-nitrosoformamide **15** via C−N_{amine} cleavage. For **9**, we predict the formation of diazotic acid **12** via retro-ene reaction *and* of the *N*-nitrosoformamide **16** via C−O cleavage. All of the decomposition reactions are predicted to be fast with activation barriers below 21 kcal·mol^{-1}.

The theoretical analysis allows for statements regarding relative yields. The C−X cleavage path of **8** is predicted to yield *more than half of the product* depending on the kinetic (81−98%) or thermodynamic (53−64%) control of its formation and considering typical error bars for chemical accuracy. In analogy, the C−O cleavage path of **9** is predicted to yield *up to half of the product* depending on the kinetic (5−61%) or thermodynamic (4−49%) control of its formation. Hence, the yield of the retro-ene reaction is predicted to be lowest for **8**. The statements made about yields assume that no intramolecular acyl transfer[42,43] occurs (**15** → **11**, **16** → **12**), and the validity of this assumption will have to be tested experimentally.

With regard to their toxicology, the theoretical analysis suggests clear differences between imines **1** and **2**. Imine **1** exclusively leads to the formation of δ-oxoalkyl diazotic acid and the diazotic acid functionality of this metabolite is responsible for adduct formation with biological materials. In contrast, imine **2** is predicted to yield large amounts of *N*-nitrosoformamide, and its capacity for adduct formation differs from that of the alternative diazotic acid. The toxicology of imine **3** falls in between.

We are exploring this chemistry in the laboratory, and we are particularly interested in the variability of the yields in a variety of solvents. The microsolvation-assisted C−X cleavage might provide a possible means to control the rate of that reaction by way of solvent changes. The theoretical analysis also clarifies the role of the NN-isomerization barrier for the determination of the product distributions. Since the NN-isomerization

(42) (a) Birman, V. B.; Uffman, E. W.; Jiang, H.; Li, X.; Kilbane, C. *J. Am. Chem. Soc.* **2004**, *126*, 12226. (b) Hess, R. A.; Hengge, A. C.; Cleland, W. W. *J. Am. Chem. Soc.* **1997**, *119*, 6980. (c) Page, M. I.; Jencks, W. P. *J. Am. Chem. Soc.* **1972**, *94*, 3263.

(43) (a) Rojas, C. M.; Rebek, J., Jr. *J. Am. Chem. Soc.* **1998**, *120*, 5120. (b) Ersoy, O.; Fleck, R.; Sinskey, A.; Masamune, S. *J. Am. Chem. Soc.* **1996**, *118*, 13077.

affects the charge distribution in the >N−N=O fragment, specific solvation might by a tool to increase the NN-isomerization barrier in more polar and/or more H-bonding solvents, and even small changes might provide large increases in products resulting from C−X cleavage.

Acknowledgment. This work was supported by grants form the National Cancer Institute (R01CA85538), the National Institutes of Health (R01GM61027), and the National Science Foundation (231354). We thank IATS (Drs. Gordon Springer and Larry Sanders) for general allocations of computer time on the University of Missouri-Columbia Research Computing Facilities.

Supporting Information Available: Documentation of the potential energy surface analyses including eight tables with total and relative energies, 12 figures of stationary structures of conformers, Cartesian coordinates of **1**−**16**, and complete citations of any abbreviated references. This material is available free of charge via the Internet at http://pubs.acs.org.

JO050856S